8. M. Morduchow and P. Libby, "On a complete solution of the one-dimensional flow equations of a viscous, heat-conducting compressible gas," J. Aeronaut. Sci., 16, No. 11, 674-684 (1949).
9. S. Rubin and P. Khosla, "Higher-order numerical solutions using cubic splines," AIAA 2nd Computation Fluid Dynamics Conference Proceedings, Hartford, CT, June 19-20, 1975 (1975), pp. 55-65.
10. B. L. Lohar and P. C. Jain, "Variable mesh cubic spline technique for N-wave solution of Burgers' equation," J. Comput. Phys., 39, 433-442 (1981).
11. Yu. A. Polyakov, "Study of heat exchange in shock wave reflection," Teplofiz. Vys. Temp., 3, No. 6, 879-888 (1965).
12. G. Emmonds (ed.), Fundamentals of Gas Dynamics [Russian translation], IL, Moscow (1963).

EFFECT OF VISCOSITY ON THE VORTEX STRUCTURE OF A FLOW AROUND A CYLINDER AND THE DRAG OF THE CYLINDER WITH AND WITHOUT A DISK IN FRONT OF IT

V. K. Bobyshev, S. A. Isaev, and O. L. Lemko

UDC 532.517.2

Large-scale vortex structures appearing in a flow around a cylinder with and without a disk for Reynolds numbers from 40 to 2500 are studied numerically and experimentally.

The use of detached flows in different practical applications, in particular, to form a forward detached zone by placing in front of a blunt body a diskotic attachment in order to reduce the head drag of the body [1], has stimulated the study of large-scale vortex structures, arising near poorly streamlined bodies, based on physical experiments in a hydrodynamic tube and computer calculations. The combination of the methods of physical and numerical modeling enabled, on the one hand, obtaining more detailed information about the characteristic features of detached flow and the effect of geometric and flow parameters on the vortex structure, and on the other evaluating the reliability of the computational method used and its ability to describe correctly the basic features of the flow pattern as well as to predict with an accuracy adequate for practical applications its integral and local characteristics. The evolution of vortex structures for Reynolds number from 40 to 2500 is studied for the example of a uniform flow of an incompressible liquid around a cylinder of elongation λ (λ = 14) with and without a thin circular disk of radius r, placed coaxially in front of the flat face of the cylinder at a distance l. Here and below all geometric dimensions are scaled to the radius of the cylinder R. In this paper attention is devoted primarily to the study of the effect of convection and diffusion on vortex formation and the determination of the relationship between the structure of detached flow around bodies and their integral and local characteristics, in particular, the head drag of blunted bodies. The velocity U and the density ρ of the incident flow are used as scaling parameters. The radius of the connecting rod is constant and equal to 0.07.

In the experimental study of an axisymmetric, low-velocity, uniform flow of air around a disk–semiinfinite-cylinder arrangement [2], performed at high Reynolds number Re of the order of 10^5, it was found that there exist optimal geometrical dimensions r_{opt} and l_{opt}, corresponding to minimum profile drag of the body. Thus, for example, for r_{opt} = 0.75 and l_{opt} = 0.75 the profile drag coefficient of a body with this shape C_{xp} = 0.02, i.e., it is close to the drag coefficient of a body with a conveniently streamlined shape. In this paper, bodies of revolution of the same configuration with optimal or close to optimal dimensions at high Reynolds numbers in a laminar flow are studied. It is especially interesting to compare the role of vortex formation in the reduction of drag of systems of poorly streamlined bodies with the case of flow around individual bodies.

D. F. Ustinov Leningrad Mechanics Institute. Translated from Inzhenerno-Fizicheskii Zhurnal, Vol. 51, No. 2, pp. 224-232, August, 1986. Original article submitted May 16, 1985.

 0022-0841/86/5102-0914$12.50

The experimental study of detached flow around models of the bodies of interest was carried out in a low-velocity (U = 0.1 m/sec), continuous-action, hydrodynamic tube of the open type whose vertical working section had a volume of 300 × 300 × 800 mm. The radius R of the cylindrical part of the models was chosen so as to minimize the effect of the blockage of the working section and of the walls of the hydrodynamic tube on the flow near the body. The disk had a thickness of 0.03. The Reynolds number of the incident flow equaled 10^3. The flow pattern was visualized by coloring flow lines with a dye (in this case inks), injected into the flow in front of the model from a special "comb." The model of the body, fastened in a holder on a coordinate setup, was placed in the working part of the tube at zero angles of attack and slipping, which ensured axisymmetric flow around the body. The physical patterns of the flows near the bodies studied was recorded by means of still and motion picture photography.

The experiments demonstrated that there exists a steady-state of the flow around cylindrical bodies, which makes it possible to use a stationary mathematical model to describe the flow. As follows from the photographs of typical patterns of detached flow around a cylinder with (a) and without (b) a disk in front of it shown in Fig. 1, developed circulation zones with detachment of the flow at the front sharp edges of the bodies – the disk in front of the cylinder in the case of the disk–cylinder arrangement or a solitary cylinder – are characteristic features of the flow structure formed. In the first case, the detachment zone is located in the space between the disk and the cylinder, the flow is attached practically at the sharp edge of the cylinder and the flow streams past the side surface of the cylinder without detachment. A very long detached zone forms on the lateral surface of the cylinder in the case of flow around a separate cylinder, and the radius of the zone is comparable to the radius of the cylinder. These circumstances must be taken into account in constructing a mathematical model by using a finite-difference grid of higher density near the points of detachment and attachment of the flow as well as shear layers on the boundaries of the circulation zones and boundary layers at the surface of the body.

The detached axisymmetric flow of an incompressible viscous liquid around a body is modeled by means of the stationary Navier–Stokes equations in natural variables, written out in the canonical divergent form in cylindrical coordinates x, y. This form of the equations is preferable for constructing a conservative finite-difference scheme, in which the laws of conservation of mass and momentum for any working cell hold to within an error equal to the round off error. The characteristic features of the starting elliptic system of partial differential equations are its substantially nonlinearity, which is associated with the dominant effect of convective transport processes at moderate and high Reynolds numbers, and the presence of a small parameter in front of the higher order derivative in the terms modeling the diffusion transport. In constructing the computational scheme these factors determine the computational stability and the effect of artificial diffusion on the solution.

The transformation from the differential equations to their difference analogs involves the use of the method of a control volume. According to this method, the starting system of equations is integrated over the volume of an arbitrary cell and the algebraic equations obtained represent the balance relations between the convective and diffusive flows through the boundaries of the cell and source terms, determined at the center of the cell. Central-difference formulas are used to approximate the diffusion flows and the derivatives in the source terms. At the same time, the analog approach to the representation of convective flows leads to a computational procedure which becomes unstable for finite-difference Reynolds numbers of $|Re_c| > 2$. In order to ensure the stability of the calculation when modeling flows with intense convective transport, first-order counterflow schemes are widely used. In schemes of this type there are no restrictions on the finite-difference Reynolds number, but their stability is ensured by introducing a significant artificial diffusion, whose coefficient of numerical viscosity depends on the size of the cell, the local velocity, and the orientation of the streamlines relative to the boundaries of the working cell. As a result, in calculations of intense flows with high Reynolds numbers and strongly curved streamlines, in particular, with detachment of the flow on real grids limited by the capabilities of the computer, the artificial diffusion often turns out to be more intense than the diffusion due to molecular viscosity, and the real transport processes are thus masked in the solution. The zones of large gradients in the flow parameters, such as shear layers, are strongly distorted, which distorts the structure of the detached flow as a whole around bodies. The undesirable effect of artificial diffusion on the solution can be reduced by introducing working finite-difference grids adapted to the structure fo the flow or by increasing the order of

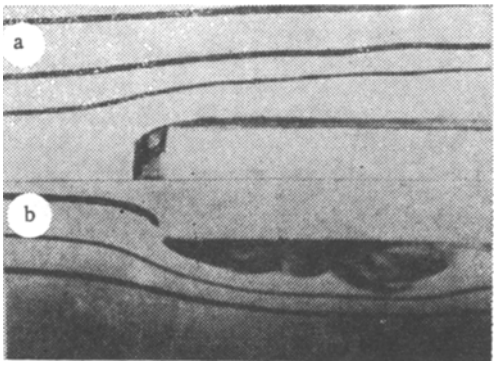

Fig. 1. Physical pattern of the structure of detached flow around a cylinder and a cylinder with a disk ($r = l = 0.70$) with $R = 1000$.

the approximation of the convective terms in the transport equations by their finite-difference analogs. Here a different approach, which is easier to implement, is used. It combines rectangular grids along the contour of the body and the quadratic upstream interpolation scheme proposed by Leonard [3] in order to describe convective transport through the boundaries of the working cell. The test of this method in [4] in a calculation of shear layers showed that the layers are described with high accuracy with quite coarse grids at high (or the order of several thousand) Reynolds numbers. Increasing the order of the approximation in Leonard's scheme involves increasing the number of nodes in the working grid. This scheme differs from the central-difference scheme in that it has an additional correction, determined by the curvature of the distribution of the dependent variable in a direction upstream from the cell boundary under study. In order to use the computational procedure in [5], based on the standard three-point in one of the coordinates, developed for first-order counterflow schemes, Leonard's original scheme is modified in a manner analogous to that in [6] so as to ensure diagonal-dominance of the matrix of coefficients in the resulting algebraic equation owing to the regrouping of terms in expressions for convective flows through the boundaries of the cell. This form enables convergence of the computational procedure without restrictions on the magnitude of the finite-difference Reynolds number.

The algorithm for solving the problem is constructed by the pressure-correction method. In the iteration process the axial u and the radial v components of the velocity are determined simultaneously from the momentum equations at the predictor stage for the conjectured pressure distribution. At the correction stage the pressure field is refined so as to ensure the conservation of mass in each working cell. Then the velocity components are corrected. The algebraic equations are solved at each iteration step by an explicit-implicit linear scanning method, which combines scalar three-point iteration in the radial direction with the Gauss-Seidel relaxation procedure in the axial direction. The convergence of the iterative process is determined by the smallness of the change in the integral and local characteristics of the flow around the body, in particular, the profile drag coefficient of the body, and it is also monitored by the discrepancy in the solution of the continuity equation.

The working region is bounded by the axis of symmetry, the surface of the cylinder in the flow, the axes of the sections oriented upstream and downstream from the face of the cylinder, and a cylindrical control surface, placed coaxially with the respect to the cylinder under study. The velocity and pressure of the incident uniform flow are given on the inlet boundary, "soft" boundary conditions are posed on the outlet boundaries, symmetry conditions are satisfied on the axis of symmetry, and sticking conditions are imposed on the solid surfaces. The inlet and outlet boundaries of the working region are located at a distance from the sharp edge of the cylinder such that the boundary conditions imposed on them would not significantly affect the structure of the detached flow and the integral force characteristics of the flow. The position of the boundaries was chosen in the course of the numerical experiments (for example, the distance from the cylindrical surface to the top boundary was set equal to 17). The calculations were performed on a strongly nonuniform grid with 90×40 and 50×36 nodes. A grid with a chess-board structure, in which the nodes for the velocity components u and v were shifted by half a step in the axial and radial directions with respect to the pressure nodes, was used. This arrangement of the nodes makes it possible to

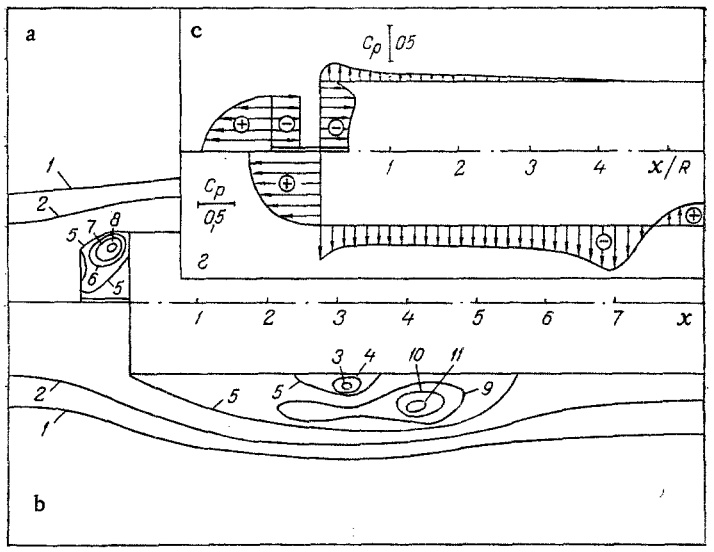

Fig. 2. Structures of the detached flow around a cylinder with (a) and without (b) a disk (r = l = 0.70) with Re = 1000 (1 – ψ = 0.99; 2 – 0.5; 3 – 0.02; 4 – 0.01; 5 – 0.0; 6 – (–0.01); 7 – (–0.03); 8 – (–0.05); 9 – (–0.1); 10 – (–0.2); 11 – (–0.3)) and the distribution of the coefficient C_p of the surface pressure along the cylinder with (c) and without (d) the disk.

avoid the oscillations of the pressure and the velocity, which arise in the calculation on a normal grid with unshifted nodes [5]. The minimum grid steps in the axial and radial directions equaled 0.02. In the calculations the disk was assumed to be infinitely thin. Twenty nodes were placed on the endface of the cylinder, eleven nodes were placed on the disk, 20 to 25 nodes were placed on the lateral surface of the cylinder, and 15 nodes were placed between the disk and the cylinder. In the region of development of the shear layer, the grid in the radial direction is nearly uniform with a step of 0.03. Six to eight hundred iterations were required in order for the solution to converge. The coefficients of lower relaxation did not exceed 0.15-0.25.

Figures 2-4 show some of the results obtained.

The streamline patterns in Fig. 2 for a laminar flow (Re = 10^3) around a semiinfinite cylinder with a flat face with (a) and without (b) a disk in front of it (r = l = 0.7) demonstrate the development of a structurally quite complicated and very strong detached flow. Both the forced (Fig. 2a) and naturally formed (Fig. 2b) detached zones contain secondary vortices. This has been observed repeatedly in the analysis of circulation flow induced in a rectangular cavern by the motion of one of its boundaries [7]. The maximum velocity of the return flow in the large-scale vortex on the lateral surface of the cylinder is of the same order of magnitude as the velocity of the incident flow, and the maximum radius of the vortex itself equaled 0.75 of the cylinder's radius. Unlike the computational results obtained using the first-order approximation scheme [8], the detachment of the flow around a cylinder occurs at the break point in the contour and not on the lateral surface of the cylinder below the sharp edge. Analysis of Figs. 1 and 2 shows that the computed configurations of the primary large-scale vortices in the flow around a cylinder with and without a disk agree with the physical flow patterns. It is interesting that the detached flow on the lateral surface of the cylinder vanishes when a disk with the optimal or nearly optimal dimensions r_{opt} and l_{opt}, which sharply (by almost a factor of 6) reduces its profile drag (see Fig. 4c), is placed in front of the cylinder. The formation of the front detached zone leads to a flow pattern on the lateral surface of the cylinder which is characteristic for a conveniently streamlined body; in addition, because of the appearance of a strong large-scale vortex in the region between the disk and the cylinder strong rarefaction appears near the sharp edge of the cylinder (see Fig. 2c). In a flow around a single cylinder a plateau with a negative pressure coefficient, which is characteristic of developed detached flows and extends from the sharp edge over several cylinder radii to the zone of the strongest return flow (near the center of the primary vortex), corresponding to a local rarefaction maximum (fig. 2d), is present on the lateral surface of the cylinder. When a disk is placed in front of the cylinder a practically isobaric flow, in which the pressure equals the pressure in the incident flow, around the lateral surface of the cylinder forms (Fig. 2c).

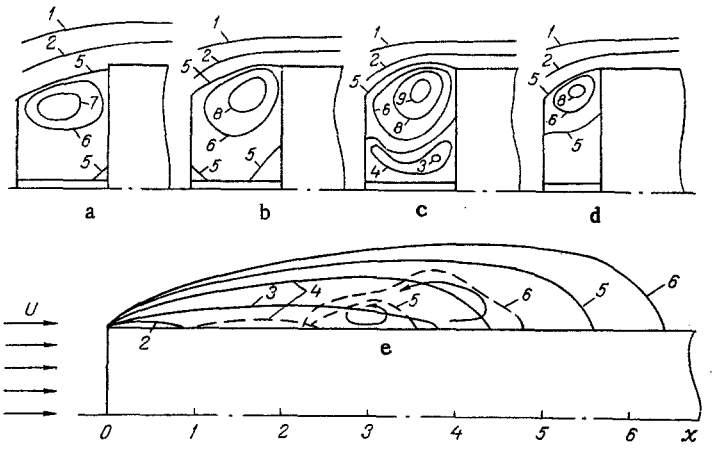

Fig. 3. Structures of the detached flow around the disk-cylinder system r = l = 0.75 (a – Re = 40; b – 500; c – 1000); r = 0.75; l = 0.5 (d – Re = 1000): 1 – ψ = 0.25; 2 – 0.1; 3 – 0.002; 4 – 0.001; 5 – 0.0; 6 – (–0.01); 7 – (–0.02); 8 – (–0.03); 9 – (–0.05) and the separating streamlines (ψ = 0) in a flow past a cylinder (e): 1 – Re = 40; 2 – 100; 3 – 250; 4 – 500; 5 – 1000; 6 – 2500 (the broken lines correspond to secondary vortices).

Figures 3 and 4 show the effect of viscosity on the vortex structure and the distribution of the local and integral characteristics of the flow around the bodies of interest. An increasing Reynolds number, which corresponds to a decrease in the effect of the diffusion-transport viscosity intensifies the detached flows, increases the size of the primary large-scale vortices, and leads to the appearance and development of secondary vortices. Thus for a disk-cylinder configuration with r = 0.75; l = 0.75 (Figs. 3a-c), as R varies from 40 to 10^2 the point of attachment of the flow moves along the end surface of the cylinder toward its sharp edge and at R = 250 the position of the dividing streamline, connecting the sharp edges of the disk and the cylinder, remains unchanged. As in the case of the evolution of a circulating flow in a deep rectangular cavern with a mobile upper boundary as Re increases [7], the growth in the corner secondary vortices leads to the formation of a radially oriented system of large-scale vortices, whose intensities, determined by the maximum magnitudes of the stream functions, differ strongly, decreasing toward the symmetry axis. The highest velocity of the return flow in the region between the disk and the cylinder increases when Reynolds number varies from 40 to 10^3 by almost a factor of 4, constituting at Re = 10^3 about 35% of the velocity of the incident flow (Fig. 4b). The development of a primary large-scale vortex as Re increases is accompanied by an increase in the rarefaction in the front detachment zone (Fig. 4a), which leads to a rapid drop in the profile drag of the arrangement (Fig. 4c). It should be noted that as Re increases the detachement zone becomes increasingly more isobaric, and the region of local increase in the pressure in the vicinity of the point of attachment of the flow becomes smaller.

For a flow around a semiinfinite cylinder with a flat end face, as in previous calculations using a first-order approximation scheme [8] no detachment was observed on the lateral surface of the cylinder for low Reynolds numbers of the order of 40 (fig. 3e). The pressure distribution on the end face and therefore the profile drag of the cylinder (Fig. 4c) in this case are also largely determined by viscous effects, and in addition the force loads are larger than in states in which the convective transport predominates. At Re = 10^2 the role of diffusion transport decreases the pressure on the front face and the drag of the cylinder decrease, and a very narrow and short circulation zone with a point of detachment lying below the sharp edge is observed on the lateral surface of the cylinder. As Reynolds number increases further the point of detachment of the flow shifts toward the sharp edge and the detachment zone on the lateral surface of the cylinder increases intensively both in the axial and radial directions, reaching at Re = 2500 almost 6.5 cylinder radii in length and 1 cylinder radius in height. At the same time, the angle between the dividing streamline and the axis of symmetry at the sharp edge increases monotonically, approaching in the limit Re $\to$ 10^3 some asymptotic value. The development of a large-scale vortex thus affects the distribution of the pressure on the front end face of the cylinder, increasing somewhat the loads in the

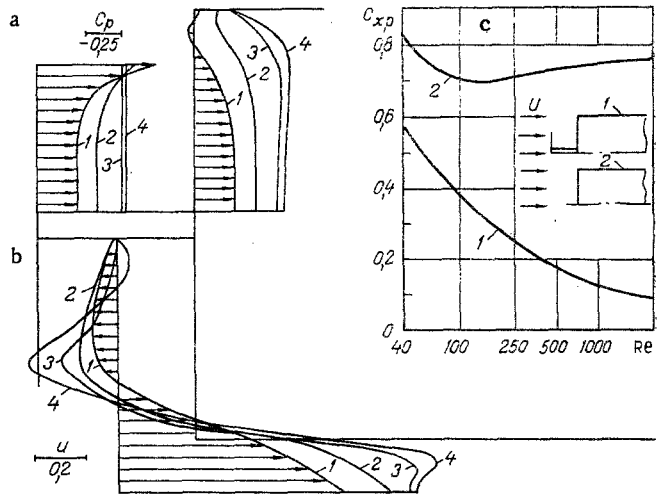

Fig. 4. Distribution of the pressure coefficient C_p on the front and back sides of the disk and on the fornt face of the cylinder (a), profiles of the axial component of the velocity in the central section (x = 0.375) of the front detached zone (b) (1 – Re = 40; 2 – 100; 3 – 500; 4 – 1000), and the dependence of the profile drag coefficient C_{xp} of the cylinder with (curve 1) and without (curve 2) the disk (r = l = 0.75) on the Re number (c).

TABLE 1. Dependence of the Drag of a Disk-Cylinder Arrangement on the Geometrical Dimensions

r=0,75		r=0,7	Re=10^3
l=0,5	l=0,75	l=0,7	λ=14
0,40	0,40	0,38	C_{xp1}
—0,35	—0,35	—0,21	C_{xp2}
—0,58	—0,62	—0,41	C_{xp3}
0,17	0,13	0,18	C_{xp}
0,19	0,24	0,18	C_{xf}
0,36	0,37	0,36	C_x

vicinity of the sharp edge. This in its turn increases the profile drag of the cylinder as the asymptotic value C_{xp} = 0.75 is approached for Reynolds numbers Re > 10^3. As a result the dependence C_{xp}(Re) for longitudinal flow around a cylinder has a characteristic minimum in the vicinity of Reynolds numbers of 100-250 (Fig. 4c). The appearance of secondary vortices on the lateral wall of the cylinder is observed at Re = 500. As the Re number increases, these secondary vortices grow in size and intensity, and the height of the vortex at Re = 2500 reaches 0.7 cylinder radii. The latter circumstance is apparently one of the factors responsible for the appearance of instability in the vortex system on the lateral wall of the cylinder, leading to a nonstationary state of the flow around the cylinder. In calculations of streaming flow past a cylinder a stationary solution could not be obtained for Re > 2500, which is in agreement with available experimental data on the restructuring of the flow for this range of Reynolds numbers.

A change in the geometric dimensions of the disk-cylinder arrangement can substantially affect the vortex structure as well as the local and integral characteristics of the flow around bodies. For fixed r, as is evident from Figs. 3c and d and Table 1, decreasing l weakens the primary large-scale vortex and increases the profile drag of the arrangement. However, for long (λ = 14) cylinders a decrease in the size of the front detachment zone with no detachment of the flow around the lateral surface is accompanied by a drop in the friction drag, and the advantage of the profile drag of the arrangement (r = l = 0.75) is thus compensated by an increase in the friction drag. The comparison of the three arrangements with respect to the drag in Table 1 shows that in spite of the difference in the separate compon-

ents, the total head drag coefficients are very close. This shows that in selecting the arrangement of a long body with a minimum head drag complex optimization is required.

NOTATION

x and y, axial and radial coordinates; R, radius of the cylinder; U, velocity of the incident flow; r, radius of the disk; l, distance between the disk and the end face of the cylinder; Δx, step in the finite-difference grid in the axial direction; u and v, axial and radial components of the velocity; ρ and μ, density and coefficient of dynamic viscosity of the incident flow; p, excess pressure relative to the pressure in the incident flow; $Re = \rho UR/\mu$, Reynolds number; $Re_c = \rho u \Delta x/\mu$, finite-difference Reynolds number; $C_p = 2p/(\rho U^2)$, pressure coefficient; $\psi = \int yudy$, stream function; C_{xp}, the profile drag coefficient; C_{xf}, coefficient of frictional drag; C_x, head drag coefficient. Indices: 1, 2, 3, quantities for the front and back sides of the disk, and the end face of the cylinder, respectively; opt denotes optimal quantities.

LITERATURE CITED

1. I. A. Belov, Interaction of Nonuniform Flows with Barriers [in Russian], Mashinostroenie, Leningrad (1983).
2. A. Roshko and K. Koenig, "Interaction effects on the drag of bluff bodies in tandem," in: Proceedings of the Symposium on Aerodynamic Drag Mechanisms, G. Sovren, T. Morel, and W. T. Mason(eds.), Plenum Press, New York (1978), pp. 253-273.
3. B. P. Leonard, "A stable and accurate convective modeling procedure based on quadratic upstream interpolation," Comp. Meth. Appl. Mech. Eng., 19, No. 1, 59-98 (1979).
4. H. R. Baum, M. Giment, R. W. Davis, and E. F. Moore, "Numerical solutions for a moving shear layer in swirling axisymmetric flow," Lect. Notes Phys., 141, 74-79 (1981).
5. S. Patankar, Numerical Methods for the Solution of Problems of Heat Transfer in Fluids and Fluid Dynamics [in Russian], Énergoatomizdat, Moscow (1984).
6. K. Kha, "Calculation of flows in diffusors in the presence of spiraling and disturbances created at the inlet," Aérokosmicheskaya Tekhnika, 2, No. 4, 74-82 (1984).
7. I. A. Belov and S. A. Isaev, "Circulating motion of a liquid in a rectangular cavern at high and moderate Reynolds numbers," Zh. Prikl. Mekh. Tekh. Fiz., No. 1, 41-45 (1982).
8. V. I. Myshenkov, "Detached flow around a cylinder with a flat end face," Izv. Akad. Nauk SSSR, Mekh. Zhidk. Gaza, No. 2, 3-10 (1979).